New Journal of Physics
The open-access journal for physics

A mode-locked nanomechanical electron shuttle for phase-coherent frequency conversion

Dominik V Scheible[1,3] **and Robert H Blick**[2,4]

[1] Center for NanoScience, Ludwig-Maximilians-Universität, Geschwister-Scholl-Platz 1, 80539 München, Germany
[2] Electrical and Computer Engineering, University of Wisconsin-Madison, 1415 Engineering Drive, Madison, WI 53706, USA
E-mail: blick@engr.wisc.edu

New Journal of Physics **12** (2010) 023019 (8pp)
Received 7 October 2009
Published 15 February 2010
Online at http://www.njp.org/
doi:10.1088/1367-2630/12/2/023019

Abstract. In this paper, we present the operation of an electron shuttle realized as a nanomechanical diode for phase-coherent frequency conversion. The mechanical response of the balanced resonator displays a hierarchy of frequency-locked resonances. We are able to achieve phase control via intrinsic frequency locking of the commensurate oscillations. By selecting the appropriate winding numbers, we can apply this nanomechanical resonator for radio-frequency conversion and rectification. The results also indicate that correlated electron shuttling and dividers for frequency combs can be realized with nanomechanical resonators.

The realization of mechanical systems on the nanoscale holds two great promises: one for engineering applications, i.e. for radio-frequency communication devices [1], and the other for testing of quantum electromechanics [2]. For both cases the key reasons to pursue nanomechanics are the sensitivity and the frequency of operation [3]. The enormous sensitivity down to the quantum limit makes nano-electromechanical systems (NEMS) also extremely promising for sensor components [4, 5].

To achieve the greatest attainable precision in reading out the displacement of such sensors, a tunneling electrode is needed. This simply demands the integration of NEMS resonators into metallic single electron transistors, as proposed earlier by Gorelik *et al* [6]. For a review of the electron shuttle see Shekhter's work [7]. Such a device was investigated in our previous work

[3] Now at Hoffmann Eitle, Patent- und Rechtsanwälte, Munich and London, Arabellastrasse 4, 81925 München, Germany.
[4] Author to whom any correspondence should be addressed.

where we recorded the electromechanical response of a metallic island placed on the tips of nanomechanical resonators [8, 9]. The principal drawback of a tunnel sensor, however, is its high impedance $\mathcal{Z}$. This commonly limits its applications in radio-frequency circuitry. Nevertheless, there are two specific approaches that allow information retrieval of high-frequency signals from nanomechanical tunneling junctions: (i) direct rectification of electromagnetic radiation and, connected to this, (ii) frequency down-conversion via mixing [10]. More precisely, mixing allows nano-electromechanical down-conversion of the desired signal. In the following, we demonstrate how to combine the two approaches by making use of frequency or mode locking in a nanomechanical resonator (NEMS).

The advantage of rectification within an NEMS resonator is that it can be directly applied for probing the ultimate sensitivity of the nanomechanical system itself. The nonlinearity required for rectification conventionally stems from the nonlinear electronic response, a nonlinear mechanical response or a combination of the two. Apart from this, rectification and mode locking in nanomechanical resonators can also be caused by an effect intrinsic to electron shuttles, as previously suggested by Pistolesi and Fazio [11]. In the following, we present studies on rectification in a laterally integrated electron shuttle based on the Pistolesi–Fazio (P&F) model.

In general, a nano-electromechanical shuttle possesses an impedance $\mathcal{Z}(R_i, C_i)$ describing the electronic properties. This impedance is tunable via the displacement-dependent resistance $R_i(x)$ and capacitance $C_i(x)$ of the junctions on the left and right sides ($i =$ left or right). While the capacitance will show a linear dependence on displacement, the resistance can show ohmic or exponential response. On the other hand, the mechanical response depends on the physical realization of the resonator, i.e. material constants and geometry, and on the amplitude of the exciting force [13]. Hence, the mechanical subsystem can also show either a linear or a nonlinear response. Finally, as discussed in the P&F model, a charge shuttle can reveal an intrinsic nonlinear response due to the variation in electron occupation $n(t)$, which in turn leads to rectification of an applied driving frequency. We note that the shuttle is not operated in the regime of Coulomb blockade.

A device with which all the above regimes can be probed is depicted in figure 1(a): a suspended single-crystalline silicon (gray) beam is machined from a silicon-on-insulator substrate with metal islands (I) placed on the extended tips of the resonator on the left and right sides [14]. This resonator combines an electron current probe with a nanomechanical degree of freedom. There are two important ingredients in the design of this particular electron shuttle: the supporting mechanical resonator is designed as (i) a TFR with (ii) asymmetrical arms holding the metallic islands in place between the source and the drain contacts. However, since the two spring constants are very similar, we can assume that they cause only a weak imbalance once a force is applied via electric fields. In addition, the TFR is operated in the linear response regime, so that the nonlinearity arises because of the shuttle mechanism [11]. Another advantage of the TFR design is that it minimizes dissipation. This gives us precise control over the mechanical properties and thus enables tuning of the mechanical Q-factor.

The TFR and the nanomechanical electron shuttle combined set the stage to validate the theoretical prediction of Pistolesi and Fazio [11] on commensurate nanomechanical modes. In electrical circuits, lasers and superconductors [12], such a behavior is called mode or frequency locking and is commonly described by the Adler equations [17]. Mode locking in a laser leads to a fixed phase between all modes. Hence, the phase noise in such a resonator is minimal. In a nanomechanical resonator, mode locking is of particular relevance for *phase-coherent*

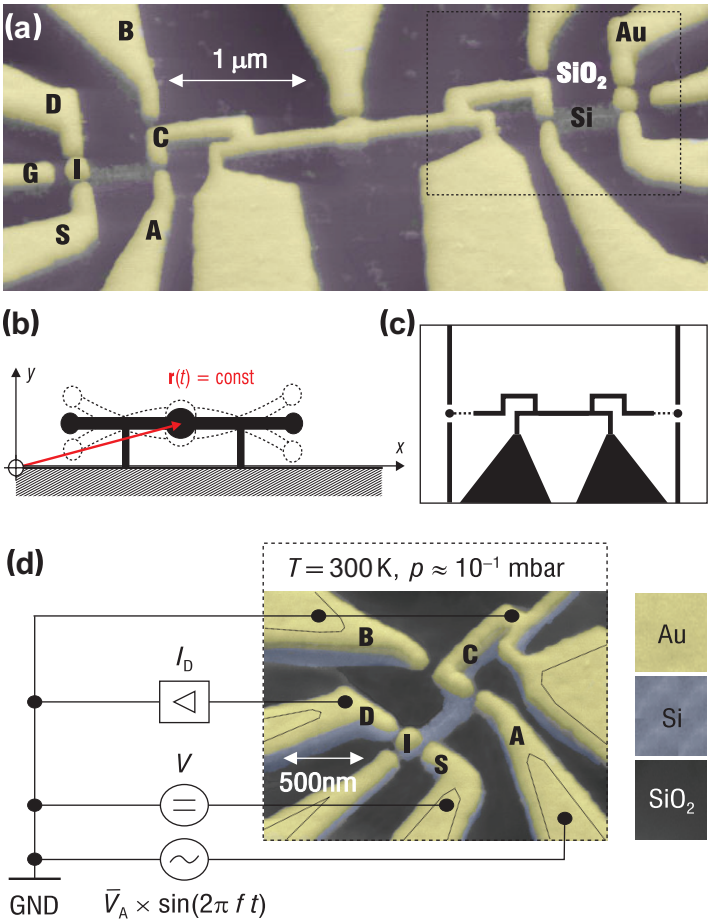

Figure 1. (a) Tuning fork resonator (TFR) with two integrated metallic islands—electron shuttles—placed on the tips of the resonator's arms on the left and right. (b) Schematics of the TFR mechanism: leaving the clamping points at rest minimizes dissipation in the resonator. (c) Sketch of the resonator indicating the wiggled resonator arms: the asymmetry of the resonator arms leads to a slight imbalance in the mechanical restoring forces if electric fields are applied to contact A or B. (d) Magnified scanning electron microscopy picture of the electron shuttle and the circuit diagram. The resonator arms or clapper are made of crystalline silicon (blue) and a thin layer of gold on the top (yellow). The clapper can be set into motion by ac/dc voltages on electrodes A and B, so that the electron island (I) shuttles electrons from the source (S) to the drain (D). The measurements are performed at room temperature in a vacuum chamber.

down-conversion of high-frequency signals with minimal added phase noise. With driving frequencies $\omega = 2\pi f$, mode locking allows us to establish a fixed relation with the eigenfrequency ω_o at $\omega \cong (q/p)\omega_o$, where q and p are integers. This is highly desired for applications such as chip-scale atomic clocks, requiring high integration density, small power levels and integration of frequency converters. In the present case, mode locking occurs as a consequence of the complex geometry of the nanoresonator, while the shuttle allows signal read-out with single electron resolution. We focus on the frequency range of 0.01–1 GHz, since down-converting GHz signals to the radio-frequency band 10–100 MHz is highly desirable.

The sketch of figure 1(b) illustrates this, where the outer tips and the center of the TFR oscillate. In earlier measurements on a fully metallized first version of a TFR [14], we have shown how to achieve this Q-control by biasing electrodes. As indicated in figure 1(a), we placed metallic islands on the tips of the TFR arms, which form two electron shuttles. Both islands have individual source, drain and gating (**G**) contacts with the distance to the source and the drain being of the order of 40 nm. The actual cantilever or 'clapper' arm (**C**) is excited capacitively via a driver signal on the electrodes (**A**) and (**B**).

Fabrication of the nanomechanical resonator is performed with optical and electron beam lithography for pattern definition on a silicon-on-insulator substrate. This enables us to carve out the central beam structure forming the TFR shown in figure 1. In a second electron beam step, we defined the electrodes and the metallic islands on the TFR's arms forming the electron shuttles. Both islands are situated between the source (S), drain (D) and gate (G) electrodes. The central part of the resonator is also covered with a thin layer of gold ($\approx$50 nm) to allow for capacitive excitation of the cantilever (C) via the electrodes (A and B). More details of the fabrication are discussed elsewhere [15, 16]. The two electron islands at the tips have dimensions of $80 \times 80 \times 50\,\mathrm{nm}^3$ with a total capacitance of $C_\Sigma \cong 22$ aF. The overall cantilever length is about 4 μm with the arm lengths of the TFR being of the order of 1 μm. As indicated in figure 1(b) the clamping points ensure that the central part and the TFR arms can vibrate freely. The layer sequence given on the right-hand side of figure 1(c) shows the top layer made of 50 nm gold based on crystalline silicon (100 nm). The sacrificial SiO_2 layer is removed in the final wet etch step, so that the TFR is suspended from its anchoring points.

To characterize the TFR's response, we measure the dc current through one of the electron islands under ac and dc voltage bias on electrode **A** while **B** is grounded. The resulting drain current I_D is amplified by an Ithaco 5820, as sketched in the circuit diagram of figure 1(c). The ac power is leveled at a maximal value of $P = -10$ dBm; this ensures that electron transport is not dominated by field emission. The ac voltage $V_\mathrm{A}(t) \propto \sin(2\pi f t)$ leads to a periodic driving force exerted onto the island, as previously described [9]. The resulting net current I_D is detected at the drain and recorded versus the ac excitation frequency f with the dc bias V_S as the parameter.

The measurements are all conducted at room temperature in a probe station; hence, no Coulomb blockade effects are expected as $k_\mathrm{B}T > e^2/C_\Sigma = E_\mathrm{C}$, where E_C is the Coulomb blockade energy. Also the driving frequencies $\omega/(2\pi) = f$ are small as compared to $E_\mathrm{C}/\hbar$. In figure 2(a) the full I_D–f spectra are given at a pressure of 10^{-1} mbar for a variety of ac excitation voltages. The fundamental mode at $\omega_\mathrm{o}/(2\pi) = 160$ MHz is indicated in the plot by the red dot. The fundamental mode is obtained from finite-element simulations. The average forward current I_D is leveled at around 16 pA, which corresponds to $n \sim 0.1$ electrons per cycle of operation at 100 MHz. This follows from $n = I_\mathrm{D}/(gef)$, where e is the electron charge, f the shuttling frequency and g the efficiency of electron tunneling, which we assume to be unity.

As seen the resonance pattern contains self-similar regions, i.e. the region below 160 MHz is similar to the one above. These resonances are superimposed on a background caused by ac rectification as predicted by the P&F model. The occurrence of these self-similar or commensurate oscillations indicates mode locking in the resonator. In figure 2(b), the mechanical resonances at the low-frequency end are plotted with the rectification current I_0 subtracted. As seen, the individual peaks' shapes indicate high Q of the TFR [18].

In figure 2(c), one island is shown on one of the TFR arms in a finite element model. We found that the wiggled resonator arm leads to two slightly different spring constants k^+ and

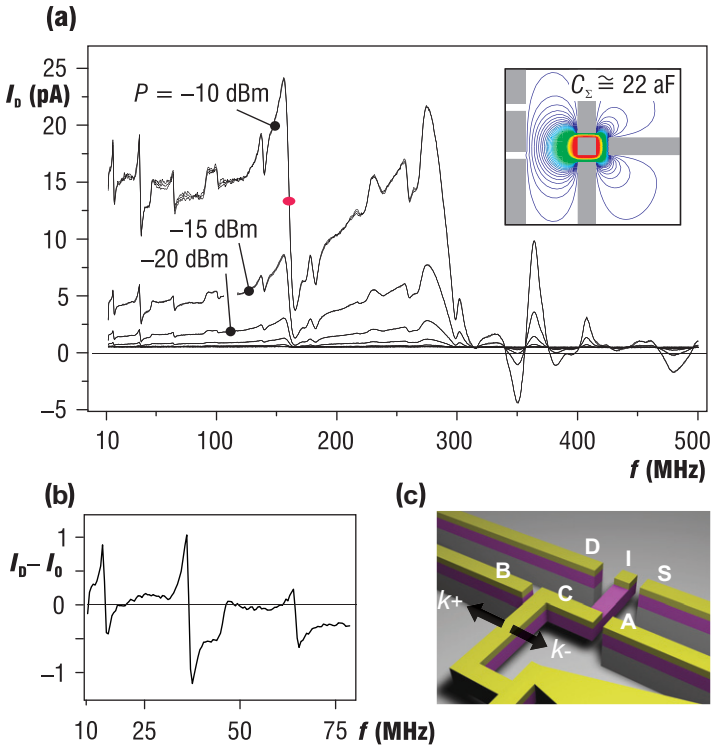

Figure 2. (a) Spectral trace of the direct current through one of the electron shuttles under ac excitation at powers from −40 to −10 dBm. The inset shows a finite element simulation of the island's total capacitance C_Σ. I–V characteristic: all the traces shown were measured three times consecutively and we did not observe any hysteresis. The red dot indicates the fundamental mechanical mode at 160 MHz. The self-similar resonances are superimposed on a dc background signal caused by rectification, which is ac power dependent. (b) Plot of the low-frequency end of the spectrum with the rectified background current subtracted, i.e. $I_D - I_0$. This underlines the high-Q value of the TFR. (c) Finite element model of one of the TFR arms with an electron island **I**. The wiggled TFR arm leads to slightly different spring constants k^+ and k^-, which lead to an imbalance under applied electric fields.

k^- depending on the cantilever's displacement toward the source or drain. We also performed a set of measurements on a macroscopic version of the TFR, in which we were able to determine this asymmetry of the spring constants (details of the measurements can be found online in [19]). This effectively leads to an imbalance of the resonator's response, as required for mode locking in an electron shuttle [11].

To probe rectification in detail, we traced the dc bias dependence of the TFR shuttle versus frequency. The corresponding measurement is shown in figure 3: in (a) the full spectrum is given, changing the bias from −50 to +50 mV at two ac powers. At a low power of −40 dBm, no mechanical resonances are excited, so that we can define the background I–V characteristic. The resulting linear dependence found is plotted in the inset, indicating that we are dealing with a linear electronic circuit. The ohmic response stems from a phenomenon called self-excitation, i.e. an applied bias leads to the occurrence of mechanical resonance even in the absence of an

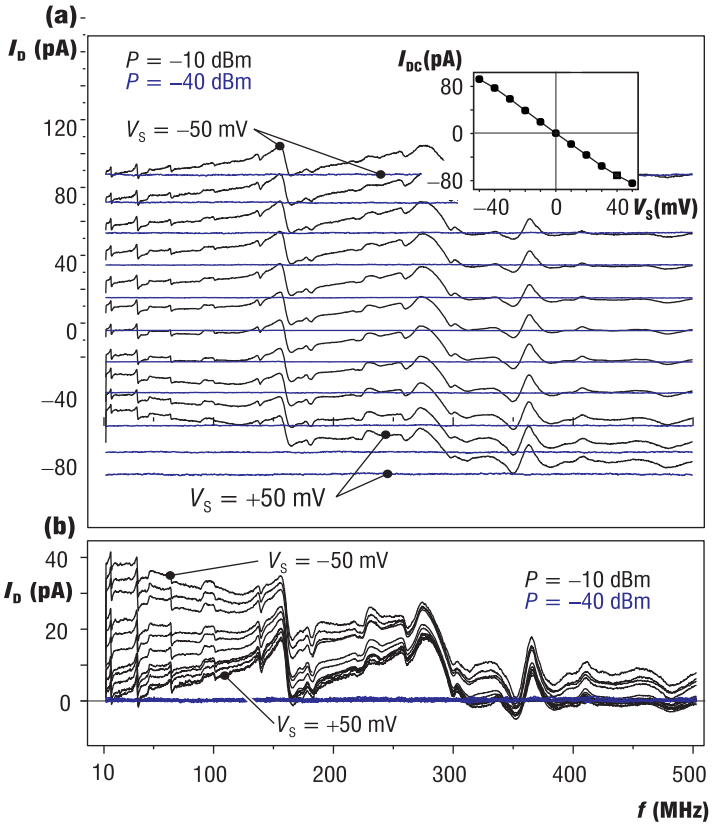

Figure 3. (a) Spectral current for different dc bias voltages at two selected ac power levels, as indicated. The details of the spectra remain identical; only the base line is shifted. The inset shows the linear IV characteristics in the static case of the electron shuttle. This current without ac excitation is due to self-excitation of mechanical resonance. (b) The same spectra as in (a), but with the linear background dc signal subtracted. The rectified part of the current is clearly seen once the ac power reaches $P = -10$ dBm. For -40 dBm, no mechanical resonances are excited.

exciting ac field. At -10 dBm the mechanical resonances re-emerge. The rectification behavior of the TFR due to the nonlinear response of the shuttle is underlined in figure 3(b), where the linear background is subtracted. Clearly, under application of ac power, rectification occurs. At -10 dBm, we find a maximal rectified dc signal of 40 pA. This response can be tuned by the dc bias as shown.

The specific resonance pattern can be fully explained within the P&F model, where a Newtonian differential equation describes the displacement $x(t)$ of this TFR shuttle:

$$\ddot{x}(t) = -\omega_o^2 x(t) - \gamma \dot{x}(t) + \frac{eV_A(t)}{mL} n(t), \tag{1}$$

where m is the mass of the resonator, ω_o is the oscillator eigenfrequency, γ is a damping coefficient, L is the distance between the two leads and $n(t)$ is the number of electrons on the island. As for a periodically driven pendulum, the force and the motion are in phase, whereas for high frequencies the motion is in opposite phase for low frequencies. For a weakly damped pendulum, the frequency at which the motion is changing from in phase $+\phi$ to the opposite phase

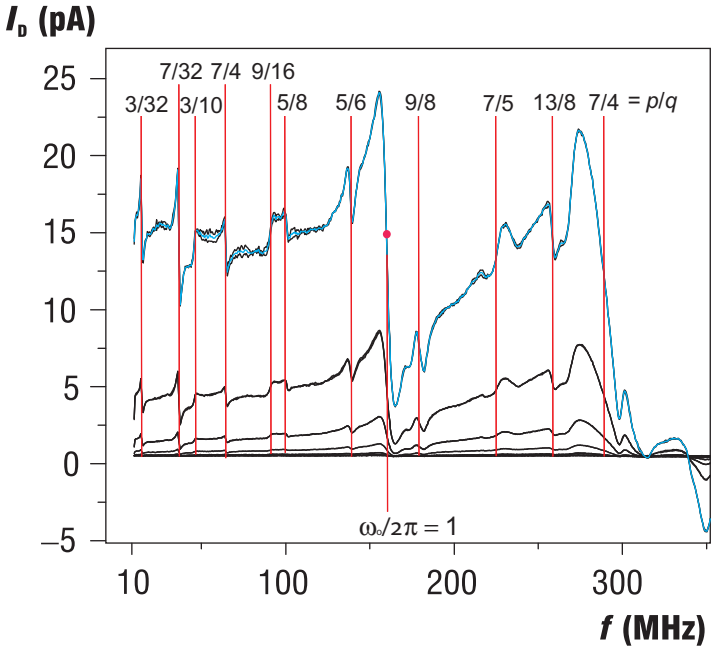

Figure 4. Plot of the resonance sequence sorted according to the fundamental mode at $\omega_o/(2\pi) = 160\,\mathrm{MHz}$ (red dot) with integer combinations p/q as indicated. The resonance at $f = 360\,\mathrm{MHz} = f_o(\frac{9}{4})$ is not shown here. Traces are measured at ac power levels from $P_{ac} = -40, -30, -20, -15$ to $-10\,\mathrm{dBm}$.

$-\phi$ is close to the resonance frequency. This leads to the current-versus-frequency behavior shown in figure 2(b). Considering mode locking, Pistolesi and Fazio found that the current spectrum can be fully mapped by the relation $\omega \cong (p/q)\omega_o$ with the integers p and q. That is, in every p periods of the electric field's oscillations, the shuttle performs q mechanical oscillations. In figure 4 the current spectra of the shuttle is depicted again with the corresponding ratios p/q noted at each resonance. As indicated, the fundamental mode was around $\omega_o/(2\pi) \cong 160\,\mathrm{MHz}$. The obtained frequencies from the given integer combinations are found to be accurate in a range of $\pm 2\,\mathrm{MHz}$ of each resonance. The results for the higher frequencies, such as the resonance at $f = 360\,\mathrm{MHz} = f_o(\frac{9}{4})$, are not shown here. It has to be underlined that for a given input frequency there exists a stable phase relation to all other (p/q)-frequencies, given by the winding number of the resonator's phase.

In summary, we have shown that a high-Q nanomechanical resonator with integrated electron shuttles can be applied for mechanically rectifying radio-frequency signals. The occurrence of commensurate mechanical oscillations enables phase coherent down-conversion to the low radio-frequency range. The results will have widespread use for quantum electromechanics, as well as for applications in sensor and communication electronics. Also, we want to stress that nonlinear NEMS contains both nonlinear nanomechanical and nanoelectronic systems. This can facilitate pumping of energy from one nonlinear circuit into the other and application as a bifurcation amplifier.

Acknowledgment

We acknowledge the support of DARPA within the CSAC program (N66001-07-1-2046).

References

[1] Rebeiz G M 2003 *RF MEMS: Theory, Design, and Technology* (New York: Wiley)
[2] Blencowe M 2004 *Phys. Rep.* **395** 159
[3] Cleland A N 2007 *Foundations of Nanomechanics* (Berlin: Springer)
[4] Roukes M L 2001 *Phys. World* **14** 25
[5] Craighead H G 2000 *Science* **290** 1532
[6] Gorelik L *et al* 1998 *Phys. Rev. Lett.* **80** 4526
[7] Shekhter R I *et al* 2007 *J. Comput. Theor. Nanosci.* **4** 860
[8] Erbe A *et al* 2001 *Phys. Rev. Lett.* **87** 096106
[9] Scheible D V *et al* 2004 *Phys. Rev. Lett.* **93** 186801
[10] Kim H S *et al* 2007 *Appl. Phys. Lett.* **91** 143101
[11] Pistolesi F and Fazio R 2005 *Phys. Rev. Lett.* **94** 036806
[12] Reinhardt C and Nori F 1999 *Phys. Rev. Lett.* **82** 414
[13] Scheible D V *et al* 2002 *Appl. Phys. Lett.* **81** 1884
[14] Scheible D V, Erbe A and Blick R H 2003 *Appl. Phys. Lett.* **82** 3333
[15] Scheible D V, Erbe A and Blick R H 2002 *New J. Phys.* **4** 86
[16] Scheible D V and Blick R H 2004 *Appl. Phys. Lett.* **84** 4632
[17] Adler R 1946 *Proc. IRE* **34** 351
[18] Scheible D V, Weiss Ch and Blick R H 2004 *J. Appl. Phys.* **96** 1757
[19] Scheible D V and Blick R H 2009 unpublished (see also http://blick.engr.wisc.edu/Experiments/macro_Q-tips.pdf)